

FLOW AND SEDIMENT TRANSPORT AROUND BANDALS UNDER LIVE-BED SCOUR CONDITION

Muhammad RASHEDUZZAMAN¹, Hajime NAKAGAWA², Hao ZHANG³, Md. Munsur RAHMAN⁴ and Yasunori MUTO⁵

¹Student Member of JSCE, Graduate Student, Graduate School of Civil and Earth Resources Engineering, Kyoto University (Yoshida-Honmachi, Sakyo-ku, Kyoto 606-8501, Japan)

²Member of JSCE, Dr. of Eng., Professor, Disaster Prevention Research Institute, Kyoto University (Shimomisu, Yoko-oji, Fushimi-ku, Kyoto 612-8235, Japan)

³ Member of JSCE, Dr. of Eng., Research Fellow, Disaster Prevention Research Institute, Kyoto University (Shimomisu, Yoko-oji, Fushimi-ku, Kyoto 612-8235, Japan)

⁴ Member of JSCE, Dr. of Eng., Associate Prof., IWFEM, Bangladesh University of Engineering and Technology, Dhaka-100, Bangladesh

⁵ Member of JSCE, Dr. of Eng., Assistant Professor, Disaster Prevention Research Institute, Kyoto University (Shimomisu, Yoko-oji, Fushimi-ku, Kyoto 612-8235, Japan).

With the aim of creating navigational channel and river bank stabilization using bandals, flow structures, suspended sediment transport pattern and bed evolution around them under live-bed scour condition were investigated in the laboratory experiment where ten pairs of such structures were installed on both sides of channel banks. The measurements were taken in dynamic equilibrium state of the experiment. A 3D numerical flow model based on unstructured mesh was developed. The model can simulate the flow structures in experiment reasonably well.

Key Words: *Bandals, dynamic equilibrium, live-bed scour, laboratory experiment, 3D numerical model*

1. INTRODUCTION

River training structures, such as groins, spur dykes etc., are frequently used to prevent river banks from erosion and improve river navigability by confining the cross-sectional area^{1,2)}. Though groins play an important role in creating navigational channel and bank stabilization, yet their expected effects are marginally quantifiable³⁾. The complex flows around groins often attack the riverbanks and in addition, it has been already proved in some developed countries where the above methods can never provide environmentally suitable solutions. Both installation and maintenance costs of groins especially for large and dynamic river are very high for the developing country like Bangladesh.

Bangladesh, which suffers from river navigability and bank erosion problem seriously, has a long history of using bandals especially to improve the preceding problem. Bandals can obstruct the flow near the water surface and divert it

towards the main channel. This characteristic feature creates deep navigational channel. As a result of the flow reduction near the river bank, they can also trap the suspended sediment in the back water zones and may protect the river bank from erosion. The working principle of bandals is based on the flow with suspended sediment. So far, the basic hydraulic functions of bandals in terms of flow and sediment control are investigated under clear-water scour condition using a very limited number of laboratory experiments by Rahman et al.,^{4,5)}. Rahman et al. explored the possibility of the formation of the navigational channel using bandals where they have conducted laboratory experiment under clear-water scour condition and developed an analytical model for the prediction of channel bed degradation and local scour depth around bandals. The limitations of these studies are the omission of the suspended sediment condition. The detailed hydraulic functions of bandals, especially flow structures and sediment transport around them under live-bed scour condition, are

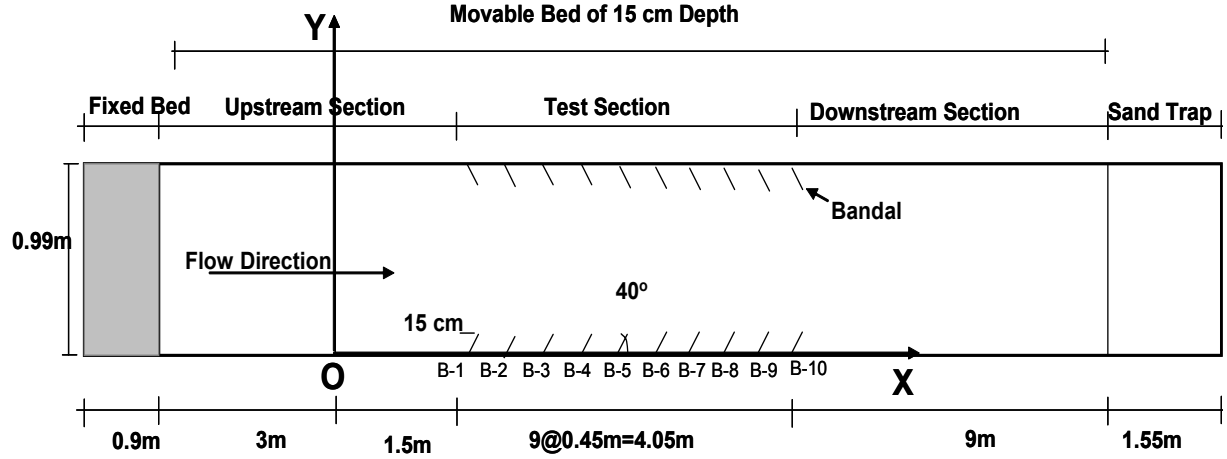


Fig.1 Overview of experimental set-up.

unknown yet. But it is very important to understand the flow structure and sediment transport around bandals for practical purposes⁷⁾.

In this research, the flow structures and bed evolution around bandals were investigated through laboratory experiment under live-bed scour condition. To simulate the flow structures, a 3D numerical model for bandals based on unstructured mesh has been developed. Finally, the simulated results are compared with experimental results.

2. LIVE-BED EXPERIMENT

(1) Experimental set-up

The experiment was conducted at the Ujigawa Open Laboratory, Disaster Prevention Research Institute, Kyoto University, in a straight tilting flume of 20 m long, 0.99 m wide and 0.30 m deep. The detailed sketch of the experimental set-up is shown in Fig. 1. There is a fixed bed, made of wooden plank, elevated 15 cm above the bottom at the upstream entrance. The purpose of the fixed bed is to smoothening the approach flow. Ten pairs of bandals are placed along both sides of the flume at an angle of 40° with downstream side bank around the middle reach of the flume. The flume bed was composed of fine sediment of mean diameter 0.11 mm with a geometric standard deviation 1.49. The bandals were non-submergible in the experiment.

(2) Hydraulic conditions

The hydraulic parameters adapted for this experiment are given in Table 1. The different parameters were designed in such a way that significant amount of suspended sediment can be generated while performing the experiment. Uniform flow condition was established by adjusting the tail gate height of the flume.

Table 1: Hydraulic conditions (equilibrium).

Parameters	Value
Discharge, Q (l/s)	17.50
Approach flow water depth, h (cm)	7.00
Channel slope, I	1/1000
Mean velocity, u (cm/s)	25.25
Sediment fall velocity, W_s (cm/s)	1.00
W_s/u_*	0.38
u_*/u_{*c}	1.97
Reynolds's number, Re	1.77×10^4
Froude number, Fr	0.53

In the table, u_* = shear velocity and u_{*c} = critical shear velocity for sediment transport, being equal to 1.33 cm/s.

(3) Dynamic equilibrium conditions

Dunes having characteristic dimension of wavelength to height ratio of the order of 10 were formed in the approach flow area. In order to attain and later on maintain the dynamic equilibrium state, a fixed amount of sediment is supplied continuously from the upstream reach of the flume. The dry sediment was mixed with water before it was supplied to avoid the dispersion effects. The reference amount of sediment supply has been estimated by using Englund – Hansen formula⁷⁾ for total load transport, but the supply amount was finally adjusted from some trial experiments. Ninety minutes were found sufficient for the attainment of dynamic equilibrium condition for this experiment.

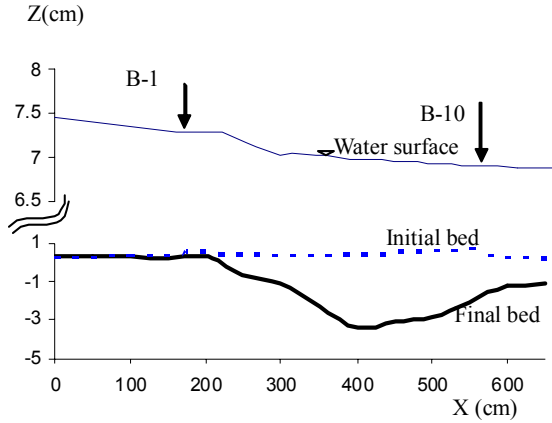


Fig. 2 Longitudinal profile of water surface and bed level along main channel.

(4) Experimental Results

After the installation of bandals, the water level in the flume shows significant increase, which is very important for navigational purpose. This is the obvious effect of the contraction in flow width by bandals. However, channel roughness has also significant contribution to the increase of the water level. Moreover, the difference in water level between upstream and downstream of the test reach is found to be around 5 mm (**Fig. 2**).

The distribution of suspended sediment concentration around bandal-4 was measured at one layer using a turbidimeter (Model PCT-3505, Tokyo Keisoku Company, Ltd.) and is shown in **Fig. 3**. Because from the trial experiments, it has been found that the hydraulic function of bandals become stable around bandal-4 and onward.

It is observed that the suspended sediment concentration is higher along the bank of the channel (maximum behind the Bandal) and reduces towards the main channel. The result is similar with that of Zhang et al.⁸⁾ who performed the live-bed scour experiment with a series of spur dykes.

The final bed contours are shown in **Fig. 4**. It can be seen that due to high velocity, the main channel was degraded and much sediment was deposited along the bank side due to the reduced velocity over there. The deposition patterns in both sides of the channel are identical. The deposition starts from the bank and is stretched towards the lateral directions upto the end of the bandals. The averaged deposition depth near the bank is about 2.5 cm.

On the other hand, the main channel degradation pattern is also very symmetrical. The first bandal gradually contracts the approach flow width and guides the flow to the main channel. After the first bandal, the contraction in flow width is constant for the rest of the test reach. That is why the main

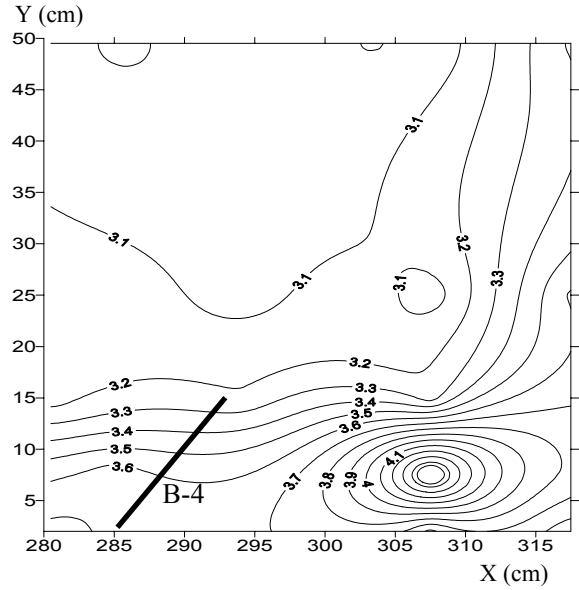


Fig. 3 Spatial variations of suspended sediment concentrations (g/l).

channel degradation is found after the first bandal and remains relatively uniform throughout the test reach.

Due to local effects channel bed around the first bandals are also eroded. The averaged main channel degradation is found to be around 3 cm for this experiment.

3. MODEL DEVELOPMENT

(1) Governing equations

The steady 3D RANS (Reynolds-averaged Navier-Stokes equation) and continuity equation were used in the proposed model which can be expressed in a Cartesian coordinate system with the tensor notation as follows.

$$u_j \frac{\partial u_i}{\partial x_j} = F_i - \frac{1}{\rho} \frac{\partial p}{\partial x_i} + \nu \frac{\partial^2 u_i}{\partial x_j \partial x_j} + \frac{1}{\rho} \frac{\partial \tau_{ij}}{\partial x_i} \quad (1)$$

$$\frac{\partial u_i}{\partial x_i} = 0 \quad (2)$$

where u_i = time-averaged velocity; x_i = Cartesian coordinate component; ρ = density of the fluid; F_i = body force; p = time-averaged pressure; ν = molecular kinematic viscosity of the fluid; $\tau_{ij} = -\rho \overline{u_i' u_j'}$, are the Reynolds stress tensors, and u_i' is the fluctuating velocity component. In the standard k- ϵ model, the Reynolds tensors are acquired through a linear constitutive equation as follow.

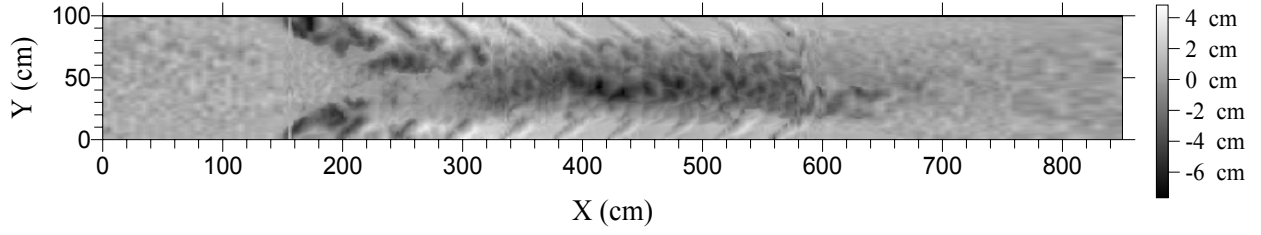


Fig. 4 Final bed contours around bandals at dynamic equilibrium state.

$$-\overline{u_i u_j} = 2\nu_t S_{ij} - \frac{2}{3} k \delta_{ij} \quad (3)$$

where k = the turbulence kinetic energy; δ_{ij} = the Kronecker delta; ν_t = the eddy viscosity and S_{ij} = the strain-rate tensor, the latter three parameters are expressed by

$$\delta_{ij} = \begin{cases} 1 & \text{if } i = j \\ 0 & \text{if } i \neq j \end{cases} \quad (4)$$

$$\nu_t = C_\mu \frac{k^2}{\varepsilon}$$

$$S_{ij} = \frac{1}{2} \left(\frac{\partial u_i}{\partial x_j} + \frac{\partial u_j}{\partial x_i} \right)$$

in which C_μ is a coefficient, being usually set to be a constant and equal to 0.09, ε is the dissipation rate of the turbulence kinetic energy k . Two transport equations as described below are employed to estimate k and ε , respectively.

$$u_j \frac{\partial k}{\partial x_j} = \frac{\partial}{\partial x_j} \left(\nu + \frac{\nu_t}{\sigma_k} \frac{\partial k}{\partial x_j} \right) + G - \varepsilon \quad (5)$$

$$u_j \frac{\partial \varepsilon}{\partial x_j} = \frac{\partial}{\partial x_j} \left(\nu + \frac{\nu_t}{\sigma_\varepsilon} \frac{\partial \varepsilon}{\partial x_j} \right) + (c_{\varepsilon 1} G - c_{\varepsilon 2}) \frac{\varepsilon}{k} \quad (6)$$

where G = the rate-of-production of the turbulence kinetic energy k , being defined as

$$G = -\overline{u_i u_j} \frac{\partial u_i}{\partial x_j} \quad (7)$$

The model constants as suggested by Rodi⁹⁾ were used, i.e. $\sigma_k = 1.0$ $\sigma_\varepsilon = 1.3$ $C_{1\varepsilon} = 1.44$ $C_{2\varepsilon} = 1.92$. For the details about the numerical model, the reference of Zhang¹⁰⁾ is suggested.

(2) Boundary conditions

The inlet boundary is considered as a Dirichlet boundary and all the quantities have to be prescribed. Since the outlet has been set as far

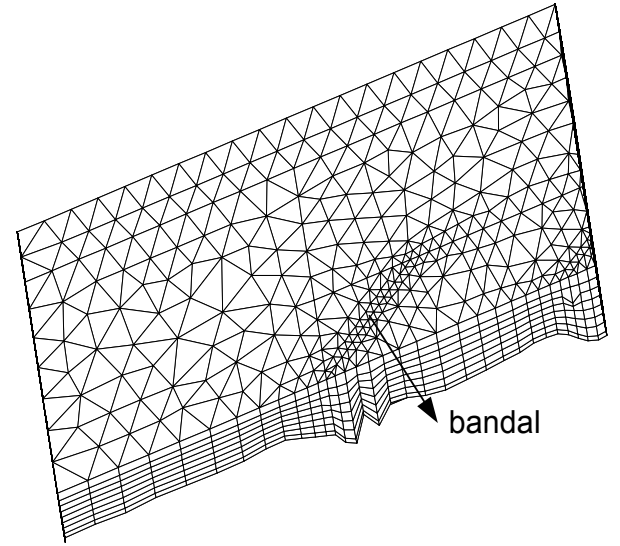


Fig. 5 Mesh system for numerical simulation.

downstream of the study domain as possible, a Neumann boundary with zero gradients is assumed at the outlet. The water surface is fixed and is considered as a symmetrical plane for the time being. Special attention has been paid for the impermeable wall boundaries. The wall function approach is preferred here to avoid the possible integration through the viscous sub-layer and to include the wall roughness more flexibly. The bandals are very complex structures. The upper part of the bandal structures are treated as impermeable wall, whereas the lower part as permeable and impermeable combination to represent the piles below the bandals. The mesh system for the numerical simulation is shown in Fig.5.

(3) Calculation Procedure

The calculation sequence is summarized as follows.

- (a) Solve the momentum equations for each velocity components, in which the pressure, the eddy viscosity, the turbulent kinetic energy and its dissipation rate are known.

- (b) The pressure-velocity coupling is treated with the SIMPLE (Semi-implicit method for pressure-linked equations) procedure. The resultant velocity field is then corrected.
- (c) Solve the transport equations for the turbulent kinetic energy and its dissipation rate and update the eddy viscosity.
- (d) Repeat the above procedures until the residual level becomes sufficiently small or the prescribed maximum iteration step is reached.

4. COMPARISON OF EXPERIMENTAL AND NUMERICAL RESULTS

The simulated flow structures were compared with those of the measured ones on the deformed fixed bed around (a) bandals-1&2, and (b) bandals-4&5 in the XY plane at $z = 4.5$ cm and (c) at the end of bandal-1 in the YZ Plane.

(1) Velocity distribution around bandals-1&2

The spatial distributions of experimental and simulated flow velocity around bandals-1&2 are shown in **Fig.6** and **Fig. 7** respectively. The magnitude of the simulated velocity agrees well with that of the experiment. When the flow approaches the first bandal, major part of the obstructed flow diverts towards the main channel, which creates a mixing zone in front of the bandal head. The rest part of the flow travels downstream through the opening at the bottom, which creates recirculating flow in-between the two consecutive bandals-1&2. The flow structures in the upstream of the bandals in both experimental and simulated results are quite identical but in the downstream it differs to some extent. A clear recirculating flow structures are very distinct while it is absence in experimental results. One reason may be the measurement grid is too coarse for the experiment.

(2) Velocity distribution around bandals-4&5

When the flow reaches around the bandal-4 where the bandal effects were found to be stable, it can be seen that both the mixing zone and recirculating flow become weak (**Fig.8 & Fig. 9**). In-between the two bandals, the velocity components of recirculating flow are found either parallel to or deflecting away from the channel bank. It means that the flow does not attack the bank and the bank is safe. This distinct feature of bandals can help to stabilize the channel bank.

(3) Velocity distribution at the end of Bandals-1.

The velocity vectors in YZ plane at the end of bandal-1 in both experimental and simulation are

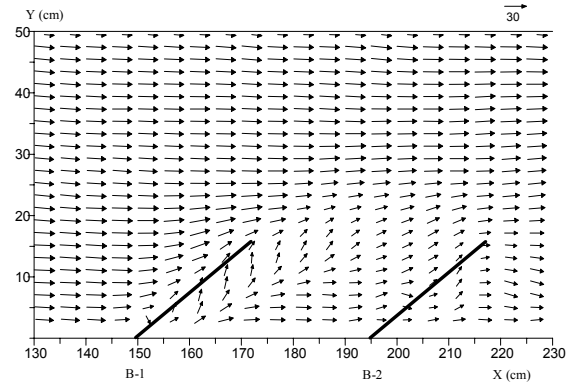


Fig.6: Velocity vector around B-1&2 (experiment).

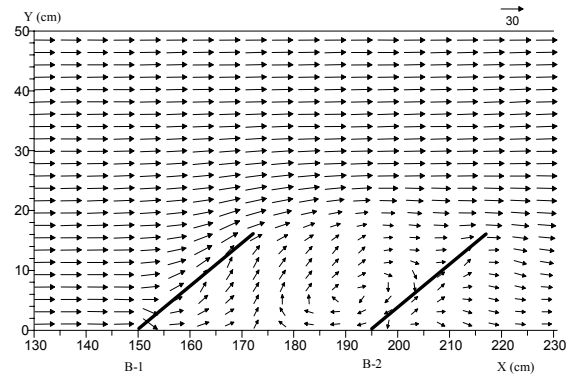


Fig.7 Velocity vector around B-1&2 (simulation).

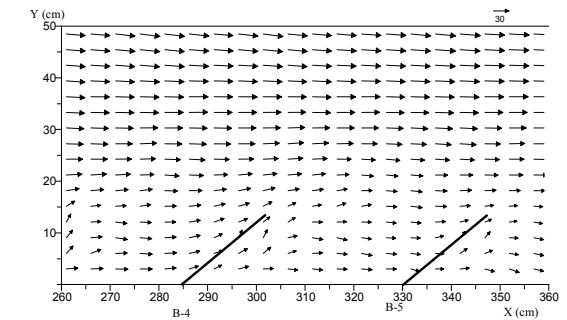


Fig.8: Velocity vector around B-4&5 (experiment).

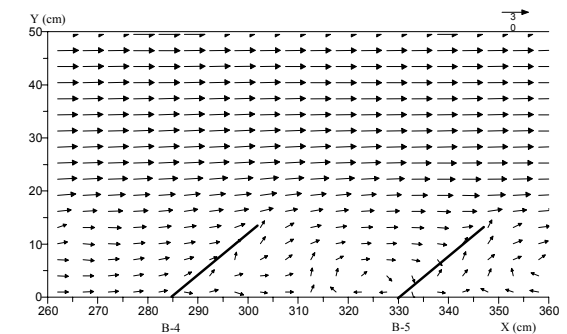


Fig.9 Velocity vector around B-4&5 (simulation).

shown in **Fig. 10 & Fig. 11**. The simulation and experimental results show clear circulation at YZ plane. However, more measurement data is needed for further analysis on the details.

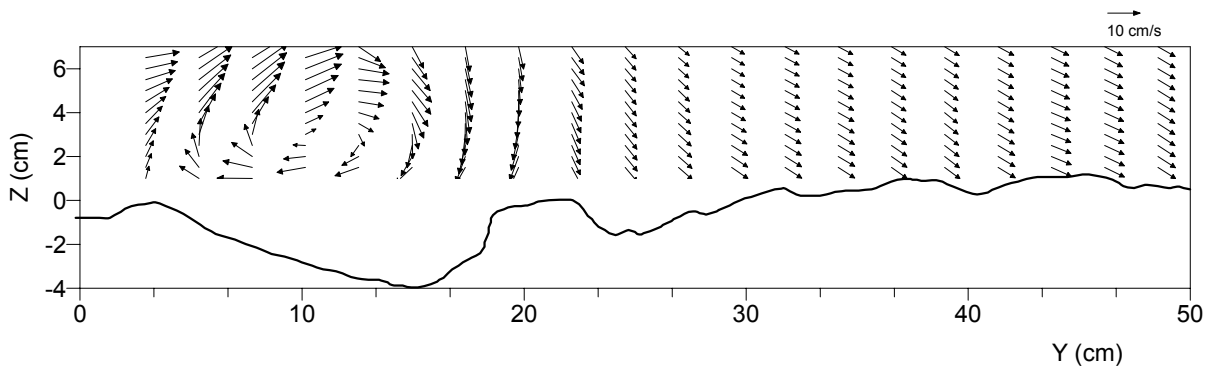


Fig. 10 Velocity distribution at the end of bandal-1 in YZ plane (experiment).

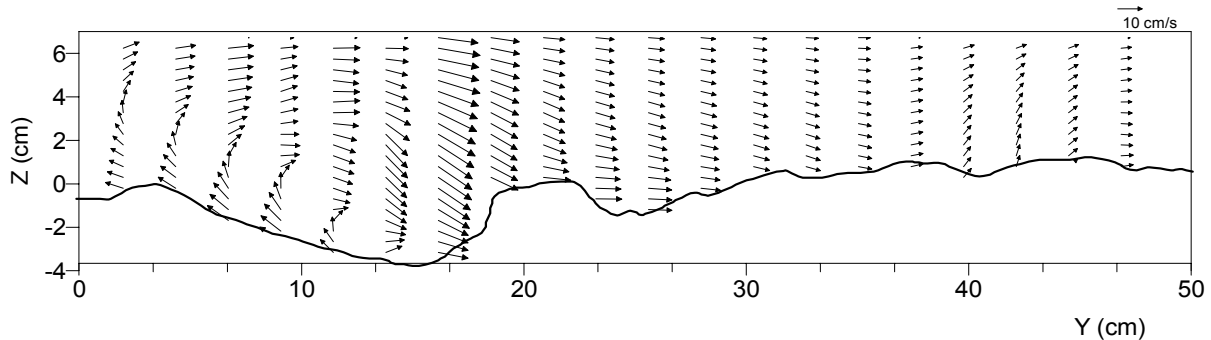


Fig. 11 Velocity distribution at the end of bandal-1 in YZ plane (simulation).

5. CONCLUSIONS

The possibility of the formation of navigational and stable channel using bandals was examined under live-bed scour condition in this study. From the experimental results, it is found that bandals can create deep navigation channel on one hand and on the other hand, they can trap sediment near the bank of the channel. Both main channel degradation and deposition near the bank are found significant. The developed model can simulate the flow structures with bandals quite reasonably well under deformed fixed bed conditions. The 3D model simulation in movable bed and comparison of the results with more experimental data are ongoing. The applications of the numerical model in different field conditions are also highly expected at the end of the ongoing research.

ACKNOWLEDGMENT

The financial support by the Monbukagakusho (Ministry of Education, Culture, Sports, Science and Technology, Japan) to the first author are acknowledged. Special thanks are due to Naoki Ito and Makoto Ano for their support while conducting the experiment.

REFERENCES

- 1) Uijtewaal, W.S.J.: Effects of groin layout on the flow in groin fields: laboratory experiment, *Journal of Hydraulic Engineering*, ASCE, Vol.131, No.9, pp.782-791, 2005.
- 2) Kadota, A., Suzuki, K. and Uijtewaal, W.S.J.: The shallow flow around a single groyne under submerged and emerged conditions, *River Flow 2006*, Vol.1, pp.673-682, 2006.
- 3) Raudkivi, A. J.: Permeable Pile Groins, *Journal of Waterway, Port, Coastal and Ocean Engineering*, ASCE, Vol.122, No.6, pp. 267-272, 1996.
- 4) Rahman, M.M., Nakagawa, H., Khaleduzzaman, A.T.M. and Ishigaki, T.: Formation of navigational channel using bandal-like structures, *Annual J. of Hydraulic Engineering*, JSCE, Vol. 49, pp.997-1002, 2005.
- 5) Rahman, M.M., Nakagawa, Ito, N., Haque, A., Islam, T., Rahman, R.M., and Hoque, M.M.: prediction of local scour depth around bandal-like structures, *Annual J. of Hydraulic Engineering*, JSCE, Vol. 50, pp.623-628, 2006.
- 6) Tominaga, A., and Matsumoto, D.: Diverse riverbed figuration by using skew spur-dike groups, *River Flow 2006*, Vol.1, pp.683-691, 2006.
- 7) Chang, H.H.: *Fluvial Processes in River Engineering*, A Wiley-Interscience Publication, John Wiley & Sons, Inc., NY, 1988.
- 8) Zhang, H. Nakagawa, H. Muto, Y. and Baba, Y.: Flow & sediment transport around groins under live bed scour condition, *Proceedings of the International Symposium on Fluvial & Coastal Disaster*, Kyoto (CD_ROM), 2005.
- 9) Rodi, W.: *Turbulence models and their application in hydraulics- a state of art review*, University of Karlsruhe , Germany, 1980.
- 10) Zhang, H.: *Study on flow and bed evolution in channels with spur dykes*, PhD thesis, Kyoto University, Japan, 2005.

(Received September 30, 2006)